3-10-2021

The Genetic Architecture of Sexual Dimorphism in the Moss

Leslie M. Kollar
University of Florida, Gainesville

Scott Kiel
Portland State University

Ashley J. James
University of Florida

Cody T. Carnley
University of Florida, Gainesville

Danielle N. Scola
University of Florida, Gainesville

See next page for additional authors

Citation Details

Kollar, L. M., Kiel, S., James, A. J., Carnley, C. T., Scola, D. N., Clark, T. N., Khanal, T., Rosenstiel, T. N., Gall, E. T., Grieshop, K., & McDaniel, S. F. (2021). The genetic architecture of sexual dimorphism in the moss *Ceratodon purpureus*. *Proceedings of the Royal Society B: Biological Sciences*, *288*(1946), 20202908. https://doi.org/10.1098/rspb.2020.2908

PROCEEDINGS B

royalsocietypublishing.org/journal/rspb

Research

Cite this article: Kollar LM *et al*. 2021 The genetic architecture of sexual dimorphism in the moss *Ceratodon purpureus*. *Proc. R. Soc. B* **288**: 20202908.
https://doi.org/10.1098/rspb.2020.2908

Received: 24 November 2020
Accepted: 2 February 2021

Subject Category:
Genetics and genomics

Subject Areas:
genetics, plant science

Keywords:
sexual antagonism, sexual dimorphism, B-matrix, constraint, G-matrix, volatiles

Author for correspondence:
Leslie M. Kollar
e-mail: lesliemkollar@gmail.com

Special Feature: Wild quantitative genomics: the genomic basis of fitness variation in natural populations edited by Susan Johnston, Nancy Chen, Emily Josephs.

Electronic supplementary material is available online at https://doi.org/10.6084/m9.figshare.c.5315502.

THE ROYAL SOCIETY PUBLISHING

The genetic architecture of sexual dimorphism in the moss *Ceratodon purpureus*

Leslie M. Kollar[1], Scott Kiel[2], Ashley J. James[1], Cody T. Carnley[1], Danielle N. Scola[1], Taylor N. Clark[1], Tikahari Khanal[1], Todd N. Rosenstiel[2], Elliott T. Gall[3], Karl Grieshop[4,5] and Stuart F. McDaniel[1]

[1]Department of Biology, University of Florida, Gainesville, FL 32611, USA
[2]Center for Life in Extreme Environments, and [3]Maseeh College of Engineering and Computer Science, Portland State University, Portland, OR 97207, USA
[4]Department of Ecology and Evolutionary Biology, University of Toronto, Toronto, Canada
[5]Department of Molecular Biosciences, The Wenner-Gren Institute, Stockholm University, Stockholm, Sweden

LMK, 0000-0001-8726-9085; ETG, 0000-0003-1351-0547; KG, 0000-0001-8925-5066; SFM, 0000-0002-5435-7377

A central problem in evolutionary biology is to identify the forces that maintain genetic variation for fitness in natural populations. Sexual antagonism, in which selection favours different variants in males and females, can slow the transit of a polymorphism through a population or can actively maintain fitness variation. The amount of sexually antagonistic variation to be expected depends in part on the genetic architecture of sexual dimorphism, about which we know relatively little. Here, we used a multivariate quantitative genetic approach to examine the genetic architecture of sexual dimorphism in a scent-based fertilization syndrome of the moss *Ceratodon purpureus*. We found sexual dimorphism in numerous traits, consistent with a history of sexually antagonistic selection. The cross-sex genetic correlations (r_{mf}) were generally heterogeneous with many values indistinguishable from zero, which typically suggests that genetic constraints do not limit the response to sexually antagonistic selection. However, we detected no differentiation between the female- and male-specific trait (co)variance matrices ($\mathbf{G_f}$ and $\mathbf{G_m}$, respectively), meaning the evolution of sexual dimorphism may be constrained. The cross-sex cross-trait covariance matrix **B** contained both symmetric and asymmetric elements, indicating that the response to sexually antagonistic or sexually concordant selection, and the constraint to sexual dimorphism, are highly dependent on the traits experiencing selection. The patterns of genetic variances and covariances among these fitness components is consistent with partly sex-specific genetic architectures having evolved in order to partially resolve multivariate genetic constraints (i.e. sexual conflict), enabling the sexes to evolve towards their sex-specific multivariate trait optima.

1. Introduction

Males and females achieve fitness through different strategies [1–3], which can drive the evolution of sexual dimorphism [4,5]. The ubiquity of sexual dimorphism suggests that selection frequently favours different trait optima in males and females. Sexual conflict occurs when an allelic substitution that increases fitness in one sex decreases fitness in the other, and thus both sexes are prevented from reaching their respective fitness optimum [6]. Theory and empirical evidence show that opposing selection in males and females can maintain genetic variation for fitness [7–15]. However, whether the sexual conflict in a population is evolutionarily transient or persistent will depend on both the nature of sex-specific selection and the nature of sex-specific genetic architecture for traits [16–20], the latter of which remains poorly understood, especially in non-model organisms.

The simplest means to evaluate the constraint imposed by a shared underlying genetic architecture for homologous traits between the sexes is to measure the

cross-sex genetic correlation (r_{mf}) [6]. A strongly positive r_{mf} for a trait will cause selection in one sex to generate a correlated response in the other sex [4,21], precluding the evolution of sexual dimorphism. Poissant *et al*. [22] found that half of the estimates of r_{mf} in 114 studies were above approximately 0.8, indicating that sexual dimorphism may often be constrained by traits having shared genetic architecture in males and females. Additional evidence for constraint on the evolution of sexual dimorphism is provided by studies identifying opposing selection gradients on correlated traits [22,23]. The resolution of sexual conflict can occur by the evolution of sex linkage or various forms of sex-biased gene expression (sex-specific genetic modifiers and genomic imprinting) [4,24–26], and allows a differential response to selection in males and females.

Single-trait analyses, however, fail to account for covariances among traits within and between the sexes, which are important for predicting the response to selection [21]. The multivariate constraint to sexual dimorphism is captured by the sex-specific genetic variance–covariance matrix ($\mathbf{G_{mf}}$), which represents a more complete framework for studying genetic architecture [18,27,28]. $\mathbf{G_{mf}}$ consists of the female- and male-specific sub-matrices $\mathbf{G_f}$ and $\mathbf{G_m}$, respectively, as well as the cross-sex cross-trait covariance matrix, $\mathbf{B}$ (and its transpose, $\mathbf{B^T}$):

$$G_{mf} = \begin{bmatrix} \mathbf{G_f} & \mathbf{B} \\ \mathbf{B^T} & \mathbf{G_m} \end{bmatrix} \tag{1.1}$$

The diagonals of $\mathbf{G_m}$ and $\mathbf{G_f}$ represent the genetic variances of the traits in males and females, respectively, and the off-diagonals within $\mathbf{G_m}$ or $\mathbf{G_f}$ are the sex-specific genetic covariances between pairs of traits. The within-trait cross-sex covariances along the diagonal of the $\mathbf{B}$ matrix can be standardized into estimates of r_{mf}, while the off-diagonal elements of $\mathbf{B}$ represent the cross-sex cross-trait covariances (i.e. covariances between a trait in one sex and a different trait in the opposite sex). While $\mathbf{G_m}$ and $\mathbf{G_f}$ are symmetric matrices, $\mathbf{B}$ is a square matrix that may not be symmetrical (i.e. $\mathbf{B}$ need not equal $\mathbf{B^T}$). Asymmetries in $\mathbf{B}$ may play an important role in the evolution of sexual dimorphism, although the prevalence of such asymmetry is unknown outside of a few model systems [20,29].

The moss *Ceratodon purpureus* is an emerging model for studying sex-specific genetic architecture. Nearly 60% of moss species have separate males and females, and sexual dimorphism is common, most notably in the production of volatile organic compounds (VOCs) [30]. *Ceratodon purpureus* females produce a wider variety and greater quantity of VOCs than males. In choice experiments with *C. purpureus*, microarthropods, such as mites and springtails, were more attracted to female than male moss VOCs [29]. Furthermore, co-cultivating mosses with microarthropods increases moss fertilization success by approximately 5 × [31]. These observations suggest that mosses and microarthropods are engaged in scent-based fertilization analogous to pollinator mutualisms in flowering plants. An increase in VOC production may attract more sperm-dispersing arthropods, enhancing both fertilization and the opportunity for mate choice [32]. In males, however, VOC production may expend resources that could be allocated to other fitness components (e.g. sperm production). Thus, the evolution of VOC production towards sex-specific fitness optima could conceivably be limited by genetic covariances between traits, sexes and trait/sex combinations.

The moss system has several technical features that make it an excellent model for sex-specific quantitative genetic analyses. The dimorphic part of the life cycle is haploid, meaning there is no dominance component of genetic variation in dimorphic traits. Sex in this system is determined at meiosis, by the segregation of the U and V sex chromosomes (as opposed to XY/ZW systems, where sex is determined at fertilization). The diploid sporophyte is always heterozygous (i.e. UV). This is because only the haploid male gametophytes make sperm, and only the female gametophytes make eggs—each chromosome is transmitted through only one sex. At meiosis, spores inheriting a U develop into female haploid gametophytes, while spores inheriting a V are males [31]. Thus, each sex contains a non-recombining sex-limited chromosome, meaning that the various asymmetries associated with the sex chromosome content in XY or ZW systems are absent [33]. Finally, the gametophytes are clonally replicable, which enables large sample sizes and limits environmental variation, increasing statistical power to estimate genetic (co)variances.

Here, we take advantage of these features to study the genetic architecture of multivariate sexual dimorphism in a natural population of the moss *C. purpureus*. We estimate $\mathbf{G_{mf}}$ and explicitly compare the male and female variance–covariance matrices, test for asymmetry in B and compare the results of single-trait and multi-trait analyses. The cross-sex correlations were heterogeneous across traits and mostly indistinguishable from zero, suggesting that the evolution of sexual dimorphism is relatively unconstrained. We detected no differences between the female and male (co)variance matrices ($\mathbf{G_f}$ and $\mathbf{G_m}$), suggesting the sexes are likely to exhibit a similar response to selection. However, this in combination with asymmetry in the $\mathbf{B}$ matrix indicates that even sexually concordant selection could generate sexual dimorphism. Nevertheless, $\mathbf{B}$ also contained symmetric components, suggesting possible ongoing sexual conflict in the form of lasting, unresolved constraints to the evolution of further sexual dimorphism.

2. Material and methods

(a) Haploid sibling family cultivation

To generate a genetically diverse sample of haplotypes to estimate the phenotypic and genetic variation in *C. purpureus*, we generated axenic cultures of 45 haploid sibling families each consisting of a minimum of three male and three female siblings [34]. These families were generated from 45 sporophytes collected in Portland, OR, with each sporophyte representing a single family. This design is analogous to genotyping the sperm from a single male in an XY system, which allows us to compare the underlying genetic architecture of male and female traits within a family and understand sex-specific differences.

To establish axenic lines from field-collected plants, we surface-sterilized operculate sporophytes and created spore solutions following published protocols [35,36]. We plated 100 µl of the spore suspension on BCD media with 0.5 mM ammonium tartrate [37]. We germinated spores under fluorescent lights (18 h dark and 6 h light) and isolated single haplotypes. We confirmed sex following Norrell *et al*. [38] and by observing sex structures.

(b) Collection of growth, development, morphology and physiology traits

We grew a total of five replicates from 345 genotypes. We grew two replicates in a greenhouse in Portland, OR. From these

plants we collected volatiles at peak sex expression, as this is when the moss was observed to be most fragrant. Following volatile collection (see below), we calculated a dry weight, analysed leaf measurements using automated methods in ImageJ and dissected tissue to confirm the presence of sex structures, measure reproductive effort and eliminate non-sex expressing profiles.

We used the remaining three replicates in a common growth chamber experiment to survey variation in growth and development. We grew each genotype on BCDA media, following Burtscher *et al*. [39]. Starting on day 0 and every 7 days after for 21 days, we collected measurements of juvenile growth (protonema) and development, including area, perimeter and circularity (a measure of how much the growth pattern deviated from a perfect circle (C; electronic supplementary material, methods equation S1)). Protonemal growth patterns in which the measured perimeter matched the estimated perimeter (assuming that the measured area was a perfect circle) return $C = 1$, while growth patterns with larger measured perimeters (e.g. more star-shaped) return values $C < 1$. Plants with circularity near 1 are largely comprised chloronema (less mature cell type). Having a larger perimeter relative to area ($C < 1$) suggests more mature, longer celled caulonema, and indicates faster maturation. Throughout this manuscript, we refer to perimeter and circularity of protonemal tissue after 21 days of growth as 'juvenile growth' and 'juvenile growth form', respectively. We also observed the accumulation of mature leafy gametophores after 21 days, recording the total number of gametophores present. We refer to the accumulation of gametophores as 'mature tissue'.

(c) Collection of volatile organic compounds

We sampled VOC emissions over 9 consecutive days using a proton transfer reaction time of flight mass spectrometer (PTR-TOF-MS 1000, Ionicon), incorporating a custom-designed sampling apparatus with hydronium (H_3O+) as the primary reagent ion (electronic supplementary material, figure S1). Prior to VOC collection, we dark-adapted replicates for 12 h and measured chlorophyll fluorescence (Opti-Sciences OP5+, Hundson, New Hampshire) to assess overall plant health and remove stressed plants from the study which could lead to outliers in VOC profiles. For each replicate, we carefully extracted 200 mg (wet weight) of mature gametophore tissue, removing remnants of soil, BCDA media, and other contaminants. We placed the plant tissue in 5 ml vials with distilled water to avoid dehydrating the plant during static head space accumulation. We placed all sample and blank cuvettes under an LED light source at 1000 PAR for two hours at 35°C. All 75 masses we report are protonated species; however, we represent volatile production as the number of different masses produced (total masses) and the total concentration of overall volatile production (total concentration).

(i) Estimating the genetic (co)variance matrix

We used a multivariate framework to estimate the extent to which the shared genome between males and females imposes a constraint on the evolution of sexual dimorphism. All of these analyses involve analysing a fitted $\mathbf{G_{mf}}$. We fitted the genetic (co)variance matrix, $\mathbf{G_{mf}}$, as a random effect in a general linear mixed-effects model (GLMM) using Bayesian Markov chain Monte Carlo (MCMC) simulations in the package MCMCglmm (v. 2.29) [40]. We fitted two models to estimate $\mathbf{G_{mf}}$: one for growth and development traits and another representing morphology and physiology traits. Our model for growth and development traits included juvenile growth, juvenile growth form and mature tissue, while the model for morphology and physiology traits included total masses produced, total concentration across all masses, relative reproductive effort and leaf length. We fitted two models because traits were collected on plants grown in different environments (growth chamber versus greenhouse) and at different stages. Thus, the categories of traits are arbitrary and titles for each model are simply for convenience. All traits in both models were zero-centred and variance-standardized across sexes. To account for sex-specific reproductive strategies, a reproductive effort was first divided by the sex-specific means (i.e. transformed to relative reproductive effort) and then zero centred and variance standardized across the sexes. Total concentration was calculated by first dividing each of the 75 detected masses by their respective means, summing the concentrations for each observation and log transforming this sum. We used MCMCglmm()'s 'trait' function to identify our multivariate list of traits in the response variable as a fixed effect (trait), which we interacted with the fixed effect of 'sex' (trait:sex) to estimate the degree of sexual dimorphism for each trait, making the full GLMM:

$$y = \text{trait} - 1 + \text{trait:sex} + \mathbf{G_{mf}} + \text{sampleID} + \text{q} + e \qquad (2.1)$$

where y is a phenotypic vector of the traits, trait − 1 indicates a model fit without an intercept, $\mathbf{G_{mf}}$ was estimated over the 45 haploid sibling families (famid), sampleID is the random effect of clonal replicate, q is an additional random effect (see below) and e is the unexplained residual variance (a Gaussian error structure was assumed for all traits). The best-fitting model (as inferred by DIC comparisons; see below) for growth and development was a three-trait (6×6 $\mathbf{G_{mf}}$) where q was 'plate', while the best fitting model for morphology and physiology was a four-trait (8×8 $\mathbf{G_{mf}}$) where q was 'date'. We modelled (co)variances using the following random effects structure of MCMCglmm: random = ~us(trait:sex): famid. Residual covariances were fixed to zero (rcov = ~idh(trait:sex): units), as male and female measures were made on separate individuals.

We used parameter expanded priors (as in Grieshop *et al*. [41]) for the growth and development model and inverse-Gamma priors (as in Puentes *et al*. [42]) for the morphology and physiology model. To determine the robustness of the posterior distribution to the prior [43,44], we compared models to other priors. The joint posterior distribution was estimated from 1 000 000 MCMC iterations after a burn-in period of 5000 iterations, and every 1000th posterior estimate was stored, providing 1000 uncorrelated posterior estimates for downstream $\mathbf{G_{mf}}$ analyses. Model convergence was assessed using Gelman & Rubin's [45] diagnostics and through visual inspection.

Because variance estimates of $\mathbf{G}$ matrices are bounded by zero, we evaluated whether (sex-specific) genetic variances were significantly different from zero via univariate model comparisons. All univariate models were fit using the inverse-Gamma priors while keeping all else equal to the respective multivariate models. Sex-specific genetic variance was detected as a δ DIC of 2 or more [46] between models with and without the 'sex' term in the random effect of $\mathbf{G_{mf}}$ (making it simply $\mathbf{G}$), and genetic variance was detected in the same way by comparing models with and without $\mathbf{G}$ (electronic supplementary material, table S1). We conducted all statistical analyses using R (v. 4.0.2; R Development Core Team 2020).

(ii) Descriptive statistics

Sex-specific genetic variances, intersexual genetic correlations (r_{mf}), and sexual dimorphisms for each trait were estimated directly by our MCMC model. Male and female genetic variances were estimated on the diagonal of the two sex-specific submatrices $\mathbf{G_f}$ and $\mathbf{G_m}$—we report the highest posterior density (HPD) mean estimates with upper and lower 95% HPD intervals as credibility intervals (CIs) in table 1. The cross-sex genetic correlations for traits, r_{mf}, were estimated along the diagonal of the *correlation* matrix for $\mathbf{B}$ (i.e. the standardized covariances, which are estimated directly by MCMCglmm())—we report the HPD

Table 1. Estimates of sex-specific genetic variance and associated 95% HPD intervals and cross-sex correlations (r_{mf}) and associated 95% HPD intervals. The degree sexual dimorphism was calculated as the difference between point estimates of male and female posterior means (male − female). A negative value for sexual dimorphism suggests the females have a larger posterior mean. All traits with an asterisk are sexually dimorphic ($p < 0.05$).

trait	female V_g	female CIs	male V_g	male CIs	r_{mf}	r_{mf} CI	sexual dimorphism
juvenile growth (*P*)	0.119	0.035, 0.207	0.247	0.114, 0.406	0.172	−0.140, 0.674	−0.026
juvenile growth form	0.148	0.061, 0.259	0.159	0.065, 0.271	0.468	0.054, 0.769	0.171
mature tissue	0.209	0.087, 0.33	0.275	0.149, 0.461	0.19	−0.138, 0.562	−0.073
total masses	0.015	0.001, 0.041	0.026	0.001, 0.067	−0.738	−0.946, 0.765	−0.487*
total concentration	0.010	0.001, 0.028	0.027	0.001, 0.067	0.799	−0.661, 0.958	0.088
leaf length	0.065	0.009, 0.143	0.122	0.026, 0.229	0.971	0.508, 0.994	−0.527*
relative repro	0.071	0.003, 0.165	0.064	0.001, 0.146	0.335	−0.739, 0.958	−0.0479

mode r_{mf} estimates with upper and lower 95% CIs (table 1). If $r_{mf} = 1$, it means that selection acting to increase a trait value in one sex would cause a correlated response of that same trait in the opposite sex (i.e. response to selection would be constrained). Consequently, an r_{mf} of zero would enable that trait to respond to sex-specific selection with no effect in the other sex. Lastly, we report the sign (male–female) and magnitude of sexual dimorphism for each trait as the HPD means and CIs for the estimated fixed effect trait:sex, with *p*-values provided by MCMCglmm() (table 1).

(iii) Similarity between $\mathbf{G_f}$ and $\mathbf{G_m}$

To compare the size, shape and orientation of $\mathbf{G_f}$ and $\mathbf{G_m}$, we calculate Hansen's difference *d* [19] and a simplified version of the eigentensor comparison [47,48]. Hansen's *d* estimates the average distance between endpoints of response vectors generated from random selection gradients on the $\mathbf{G_f}$ and $\mathbf{G_m}$ matrices [19], similar to a random skewers method [49]. An eigentensor analysis [50,51] comparing two symmetric matrices reduces to a simple difference between the matrices. Thus, we obtained an estimate of the difference between $\mathbf{G_f}$ and $\mathbf{G_m}$ by taking the difference between the 1000 paired posterior estimates of $\mathbf{G_f}$ and $\mathbf{G_m}$ and calculating the trace (sum of the eigenvalues) of this difference matrix. We report the HPD mode and 95% CIs of that trace. A test of the significance of this difference was obtained by comparison to that of a null distribution, which was generated by randomly swapping the sex labels of the 1000 paired $\mathbf{G_m}$ and $\mathbf{G_f}$ estimates. With the mode of these null estimates being very near zero and the true estimate being positive, the two-tailed *p*-value is simply the proportion the 1000 posterior estimates of the true difference that were < their respective null estimates of the difference, times two [41]. The eigentensor comparison of $\mathbf{G_f}$ and $\mathbf{G_m}$ provided qualitatively similar results (see electronic supplementary material, figure S2).

(iv) Symmetry of B

Asymmetry in the **B** matrix indicates differences in the underlying genetic architecture for traits between males and females [50,51]. For example, an off-diagonal element of **B** with a covariance of 1 between trait *i* in males and trait *j* in females would suggest that selection on trait *i* in males would cause a correlated response to trait *j* in females. Asymmetry in **B** means that selection on trait '*i*' in females will produce a correlated response on trait '*j*' in males, but that correlated response differs if the sexes are reversed (i.e. selection on trait *i* in males produces a different correlated response in females). Thus, the relative proportion of **B** that is symmetric versus asymmetric reveals the relative magnitude of cross-sex cross-trait pleiotropic constraints versus sex-specific genetic architecture, respectively. Thus, we partitioned **B** into its symmetric and asymmetric (or skew symmetric) components using matrix decomposition [29,52]. Any square matrix—**A** (e.g. **B**)—is the summation of the two components **S** and **N**:

$$\mathbf{A} = \mathbf{S} + \mathbf{N} \tag{2.2}$$

the symmetric and asymmetric components, respectively, where $\mathbf{S} = \frac{1}{2}(\mathbf{A} + \mathbf{A}^T)$ and $\mathbf{N} = \frac{1}{2}(\mathbf{A} - \mathbf{A}^T)$. The proportions of **B** that are symmetric and asymmetric are given by the ratio of the sums of squares of those components to that of the total, **B** [51,52]. We report the HPD mode and 95% CIs for these proportions by resampling them from the 1000 stored posterior estimates of **B**.

(v) Antagonistic and concordant genetic variation

To evaluate the relative proportion of genetic variation in this population that would respond to sexually concordant versus sexually antagonistic selection, we estimated the matrix $\mathbf{G_{ca}}$, following Sztepanacz & Houle [52]. The sub-matrices of $\mathbf{G_{ca}}$, $\mathbf{G_a}$ and $\mathbf{G_c}$ predict the response of the sex difference in trait values to the sexually antagonistic selection and the response of trait means to the sexually concordant selection, respectively. We projected $\mathbf{G_{mf}}$ onto a set of arbitrary orthonormal vectors ($\mathbf{S}_m$) that spanned the concordant and antagonistic subspaces of $\mathbf{G_{mf}}$. If an *n*-trait $\mathbf{G_{mf}}$ has 2*n* dimensionality (e.g. 8 in the case of the four-trait morphology and physiology matrix), then $\mathbf{S}_m$ was constructed by first taking the set of *n* eigenvectors that span the space of an *n*-dimensional identity matrix, dividing them (arbitrarily) by the square root of two (giving $\mathbf{E}_m$) and arranging them into the following 2*n*-dimensional matrix: $S_m = \begin{bmatrix} \mathbf{E}_m & \mathbf{E}_m \\ \mathbf{E}_m & -\mathbf{E}_m \end{bmatrix}$. The unit-length vectors of the first *n* columns of $\mathbf{S}_m$ therefore span the sexually concordant subspace of $\mathbf{G_{mf}}$ and the unit-length vectors of the second n columns of $\mathbf{S}_m$ span the sexually antagonistic subspace of $\mathbf{G_{mf}}$ [52]. $\mathbf{G_{mf}}$ was projected onto this space:

$$\mathbf{G_{ca}} = \mathbf{S}_m^T \mathbf{G_{mf}} \mathbf{S}_m, \tag{2.3}$$

where the upper-left and bottom-right *n*-dimensional sub-matrices of $\mathbf{G_{ca}}$ are covariance matrices that represent the sexually concordant ($\mathbf{G_c}$) and sexually antagonistic ($\mathbf{G_a}$) subspaces of $\mathbf{G_{mf}}$, respectively [52]. The proportion of $\mathbf{G_{mf}}$ that is sexually concordant and sexually antagonistic is therefore given by the ratio of the trace of $\mathbf{G_c}$ to $\mathbf{G_{mf}}$ and $\mathbf{G_a}$ to $\mathbf{G_{mf}}$, respectively [52]. Again, we report the HPD mode and 95% CIs for these overall proportions, as well as for each eigenvector of $\mathbf{G_{mf}}$, $\mathbf{G_c}$ and $\mathbf{G_a}$, by resampling the 1000 stored posterior estimates of $\mathbf{G_{mf}}$.

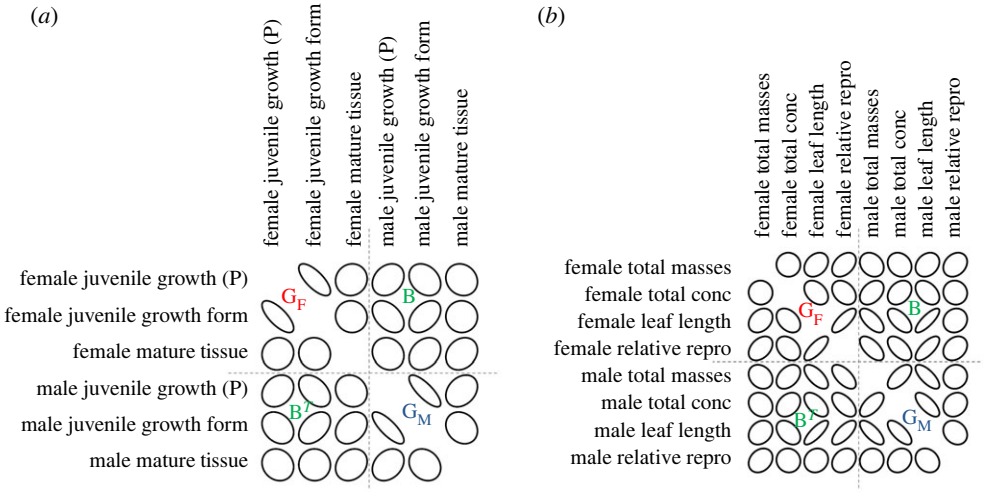

Figure 1. Genetic correlations ($\mathbf{G_{mf}}$) among traits within and between males and females represented by ellipses. A narrow ellipse is representative of a stronger correlation while a wider ellipse depicts a weaker correlation. A represents the genetic correlations between growth and developmental traits whereas B represents the correlations between morphology and physiology traits.

3. Results

(a) Sex-specific genetic variances, r_{mf} and sexual dimorphism

We found that leaf length and total masses were sexually dimorphic in our multivariate models. The sign (male–female) and magnitude of sexual dimorphism for each trait are reported as the HPD means and CIs estimated by the trait : sex fixed effect (table 1). We identified non-zero genetic variance in all traits, and non-zero sex-specific genetic variance in all traits except leaf length (electronic supplementary material, table S1). Male and female genetic variances were estimated on the diagonal of the two sex-specific sub-matrices $\mathbf{G_f}$ and $\mathbf{G_m}$—we report the HPD mean estimates and 95% CIs in table 1. The magnitude of sex-specific genetic variances ranged from 0.1 to 0.2 in growth and development and 0.001 to 0.1 in morphology and physiology (table 1). Many of our estimated genetic covariances were strong but accompanied by large uncertainties (electronic supplementary material, figures S4 and S6) which is not uncommon [40]. Juvenile growth form and leaf length had positive r_{mf} estimates with CIs that did not include zero (table 1).

(b) Comparing $\mathbf{G_m}$ and $\mathbf{G_f}$

We used two methods to assess the overall similarity between the male and female (co)variance sub-matrices $\mathbf{G_m}$ and $\mathbf{G_f}$. Hansen's difference d indicated that there were broadly no differences between $\mathbf{G_m}$ and $\mathbf{G_f}$ in terms of their multidimensional size, shape or orientation for growth and development traits ($d = 0.094$, CIs: −0.043, 0.228) or morphology and physiology traits ($d = 0.062$, CIs: −0.005, 0.129) (figure 1 and table 2). The simplified eigentensor analysis (as well as the formal version, electronic supplementary material, figure S2) showed that $\mathbf{G_m}$ and $\mathbf{G_f}$ were similar for both growth and development traits (difference = −0.173, CIs: −0.544, 0.121, $p = 0.284$) and morphology and physiology traits (difference = −0.073, CIs: −0.269, 0.091, $p = 0.24$) (figure 1 and table 2).

(c) Analysing B

We estimated symmetry and asymmetry in the **B** matrix by comparing the off-diagonal elements. Across growth and development traits, the proportion of the **B** matrix that was asymmetric was 0.112 (CIs: 0.002, 0.448) and the proportion that was symmetric was 0.884 (CIs: 0.552, 0.998) (figure 1*a* and table 2; electronic supplementary material, figures S3 and S4). Across morphology and physiology measurements, the proportion of the **B** matrix that was asymmetric was 0.312 (CIs: 0.064, 0.513), and the proportion that was symmetric was 0.688 (CIs: 0.487, 0.936) (figure 1*b* and table 2; electronic supplementary material, figures S5 and S6).

(d) Concordant and antagonistic subspace of $\mathbf{G_{mf}}$

For growth and development traits, proportionally 0.367 (CIs: 0.248, 0.476) of the total genetic variances laid within the antagonistic subspace while proportionally 0.633 (CIs: 0.524, 0.752) of the total genetic variances laid within the concordant subspace (table 2). For morphology and physiology traits, 0.241 (CIs: 0.121, 0.466) of the total genetic variances laid within the antagonistic subspace while 0.759 (CIs: 0.534, 0.879) laid within concordance subspace (table 2).

We plot the genetic variances for the eigenvectors of the concordant ($\mathbf{G_C}$) and antagonistic ($\mathbf{G_A}$) subspaces alongside that of $\mathbf{G_{mf}}$ for both growth and development traits and morphology and physiology traits in figure 2. For the growth and development traits, the genetic variances of the first two out of six eigenvectors of $\mathbf{G_{mf}}$ were fully accounted for by sexually concordant genetic variance (i.e. the first two eigenvectors of $\mathbf{G_C}$), and the third eigenvectors of $\mathbf{G_{mf}}$ was only partly explained by sexually concordant genetic variance (figure 2*a*). The remaining unexplained genetic variances in $\mathbf{G_{mf}}$'s third eigenvector is apparently sexually antagonistic, as indicated by the overabundance of genetic variance in the first eigenvector of $\mathbf{G_A}$ relative to the fourth eigenvector of $\mathbf{G_{mf}}$, and so on. By contrast, for the morphology and physiology traits, only the first one out of eight eigenvectors of $\mathbf{G_{mf}}$ were fully accounted for by sexually concordant genetic variance (i.e. the first eigenvectors of $\mathbf{G_C}$), and all remaining eigenvectors of $\mathbf{G_{mf}}$ had some fraction of their genetic variances comprised SA genetic variance ($\mathbf{G_A}$; figure 2*b*).

4. Discussion

Mosses engage in scent-based fertilization in which female plants use specific VOCs to attract sperm-dispersing

Table 2. Summary table with estimates and corresponding 95% HPD intervals and *p*-values where applicable. Estimates include comparisons between $\mathbf{G_m}$ and $\mathbf{G_f}$ (Hansen's difference *d* and simplified eigentensor analysis), asymmetry and symmetry of **B**, and proportion of antagonistic and concordant subspace relative to the total genetic variance in $\mathbf{G_{mf}}$.

model	Hansen's difference (*d*)	simplified eigentensor	proportion asymmetry B	proportion symmetry B	G_{ca} antagonistic	G_{ca} concordant
growth and development	0.094 (−0.043, 0.228)	−0.173 (−0.544, 0.121) $p = 0.284$	0.112 (0.002, 0.448)	0.884 (0.552, 0.998)	0.367 (0.248, 0.476)	0.633 (0.524, 0.752)
morphology and physiology	0.062 (−0.005, 0.129)	−0.073 (−0.269, 0.091) $p = 0.24$	0.312 (0.064, 0513)	0.688 (0.487, 0.936)	0.241 (0.121, 0.466)	0.759 (0.534, 0.879)

microarthropods, thereby increasing sexual reproduction [30–32]. Male mosses, in contrast, appear to produce fewer compounds, and in lower abundances, suggesting that VOC production may undergo sexually dimorphic selection [30,31]. Here, we used a multivariate approach based on field-collected, natural crosses to estimate the genetic architecture of variation in VOC production and life-history traits in the moss *C. purpureus*. The study population contained genetic variance for all traits, consistent with previous studies of life-history traits in other populations [34,53]. We found clear evidence for sexual dimorphism in the total number of masses produced and leaf length. Most traits have cross-sex correlations that were indistinguishable from zero, which would suggest that selection on one sex would elicit at most a modest response in the other sex. However, both Hansen's *d* and the simplified eigentensor analysis showed that the multi-trait genetic (co)variance matrices, $\mathbf{G_f}$ and $\mathbf{G_m}$, were aligned, which would intuitively suggest that the multivariate pleiotropic constraints to the response to selection would be shared between the sexes. Still, the cross-trait cross-sex genetic (co)variance matrix (**B**) had asymmetric elements, indicating some opportunity for sex-limited responses to selection in spite of the putative multivariate genetic constraints indicated by the similarity between $\mathbf{G_f}$ and $\mathbf{G_m}$.

The constraint on the continued evolution of sexual dimorphism is typically evaluated by estimating the cross-sex correlations (r_{mf}) between homologous traits, and indeed the overall mixed r_{mf} values we found here are consistent with estimates from other populations of *C. purpureus* [50]. We found no relationship between r_{mf} and sexual dimorphism further supporting the inadequacy of r_{mf} as a metric of constraint. For example, total masses were sexually dimorphic but had a nearly zero r_{mf} while leaf length was similarly dimorphic and had a high non-zero r_{mf} (table 1). Additionally, juvenile growth form was not sexually dimorphic yet had a high non-zero r_{mf}. In other populations of *C. purpureus*, McDaniel [34] found a different relationship between dimorphism and r_{mf}, suggesting that this relationship may be highly population dependent. While diploid organisms may resolve constraints to sexual dimorphism via sex-specific dominance effects [14,54,55], conflict resolution in this haploid moss may be limited to alternative mechanisms such as sex linkage- or sex chromosome-mediated gene regulation. We suspect that a key factor explaining the mix of r_{mf} values in *C. purpureus* is the fact that females and males each have a large sex-limited chromosome (U: 3450 genes and V: 3411 genes, respectively) [56], where the U is passed from mother to daughter and the V from father to son, which could enable a rapid resolution to sexual conflict. If so, this could mean that U- or V-linked variants may represent evolutionary changes aimed at resolving autosomal sexual conflict.

It is widely appreciated that single-trait analyses, like r_{mf} may fail to capture the true underlying constraint on the evolution of sexual dimorphism. Indeed, estimates showing that male and female genetic (co)variance matrices are similar suggest that the response to selection of one sex could be quite similar in the other in spite of the low cross-sex correlations for individual homologous traits. Similar to findings in other studies [50,52,57–59], we found that the overall genetic (co)variance structure was similar between males and females (table 2). Despite similar sex-specific covariance matrices, there are some observable differences, including the negative covariance of leaf length and total masses in males

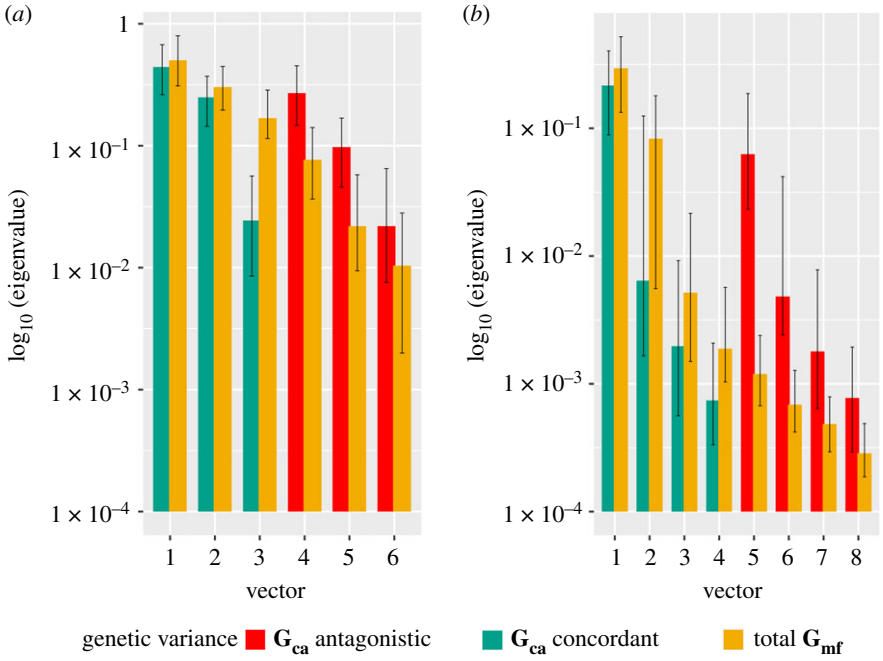

Figure 2. A comparison of the genetic variance of $\mathbf{G_{mf}}$ against the concordant and antagonistic subspaces. The height of each bar represents the estimated genetic variance for each eigenvector while the error bars show the 95% HPD. Plot (*a*) (6 dimensions) represents the growth and development traits, and plot (*b*) (8 dimensions) represents the morphology and physiology traits. (Online version in colour.)

but not females, and reproductive effort and leaf length positively covary in females but not in males (figure 1). Many of the most differentiated covariances involved leaf traits and relative reproductive effort with VOC production in mature plants. The fact that many traits show cross-trait covariances that are sexually dimorphic suggests that genetic control is both highly pleiotropic (between traits) and potentially involves strong epistatic interactions with loci on the U and V sex chromosomes. In addition, this suggests that similar patterns of selection acting on males or females could generate different phenotypic responses, potentially increasing or decreasing the population-level sexual dimorphism.

Intuitively, it would make sense that the similarity between $\mathbf{G_f}$ and $\mathbf{G_m}$ would impose a genetic constraint. However, Cheng & Houle [20] demonstrated that similarity in male and female covariance matrices coupled with some degree of **B** matrix asymmetry suggests a greater opportunity for sexual dimorphism in response to sexually concordant selection than to sexually antagonistic selection. Thus, our estimates of the proportion of standing genetic variation that could respond to sexually antagonistic selection represent lower bounds for the potential sexually dimorphic response, as further sexual dimorphism could evolve in response to sexually concordant selection. We therefore base our findings regarding multivariate genetic constraint on the estimated proportions of asymmetry and symmetry on our **B** matrix analysis [51,52].

Though **B** was largely symmetrical, indicating multivariate constraints to sexual dimorphism, a portion of the **B** matrix was asymmetric in both trait categories (growth and development and morphology and physiology). If the **B** matrix were completely symmetrical, the response to selection on males would be manifest in both the male and female offspring of the following generation. By contrast, asymmetry in the off-diagonals of the **B** matrix means that the multivariate responses to selection between males and females can be different [29,50,59,60]. The asymmetry in **B** likely results from sex-biased gene regulation mediated by epistatic interactions between autosomal variants and the U and V sex chromosomes (possibly also mediated by epigenetic factors; see Wang *et al*. [61]). There seems to be at least a putative difference between the growth and development traits and the morphology physiology traits in the degree of **B** asymmetry (table 2), which is also visually apparent in figure 1. The levels of **B** asymmetry that we find in the growth and development traits and morphology physiology traits is towards the lower and upper end, respectively, of the range of estimates among populations of *Drosophila serrata* [51], which ranged from approximately 15% to 30% (table 2). This possibly suggests a richer history of sex-specific and/or sexually antagonistic selection in morphology and physiology traits relative to growth and development traits, triggering the evolution of resolved genetic constraints.

An analysis of the degree of multivariate sexually antagonistic genetic variation in $\mathbf{G_{mf}}$ provides insight to the capacity for further response to sexually antagonistic selection [20,52]. The overall percentages of sexually antagonistic genetic variance were estimated with wide, highly overlapping CIs between our two trait categories (table 2). However, the eigenvector-specific analysis showed a greater proportion of sexually antagonistic genetic variance comprising the eigenvectors of $\mathbf{G_{mf}}$ in morphology and physiology traits relative to the growth and development traits. Further, that sexually antagonistic genetic variance was dispersed across proportionally more of the eigenvectors relative to that exhibited by the growth and development traits (figure 2). Indeed, 25–35% of the multivariate genetic variance in our population was sexually antagonistic (table 2), considerably more than, for example, the multivariate genetic architecture of wing morphology in *D. melanogaster* (4.32% sexually antagonistic genetic variance [52]). Thus, our morphology and physiology traits may possess a greater opportunity to respond to sexually antagonistic selection than the growth and development traits, echoing the greater proportion of the **B** matrix that was found to be asymmetric

relative to that of growth and development traits (figure 1 and table 2).

The rich bouquet of VOCs produced by this population may contribute to variation in attracting sperm-dispersing arthropods, with potentially major fitness consequences. Both females and males contain genetic variation for VOC production, but the structure of covariation in the sexes is sufficiently different such that sex-specific coevolution between the moss scents and arthropod behaviours could play a major role in the maintenance of genetic variation for fitness in natural populations of *C. purpureus*. The complexity of the underlying genetic architecture also highlights the potential for scent-based fertilization to contribute to pre-zygotic speciation barriers in mosses, much like the role pollination plays in angiosperms. For example, mosses may evolve suites of VOCs which match the preferences of the local mesofauna. Odour-mediated fertilization could promote the evolution of pre-zygotic isolation if moss VOCs elicit species-specific responses from sperm-dispersing microarthropods or other members of these communities. It is possible that the interaction involves additional microbial partners upon which the mesofauna feed—indeed, mosses appear to host diverse sex- and species-specific microbiomes [62–64]. Collectively these results highlight how ecological interactions may shape the evolution of sexual dimorphism [65,66], which may in turn contribute to the maintenance of genetic variation in fitness and the evolution of reproductive isolation.

Data accessibility. Data and scripts to reproduce the results of the study are available on the Dryad Digital Repository: https://doi.org/10.5061/dryad.59zw3r266 [67].

Authors' contributions. L.M.K. led the study. L.M.K, T.N.R and S.F.M designed the study. L.M.K. collected the data, with assistance from T.N.C., T.K., A.J.J., D.N.S. and C.T.C. for the life-history traits, and E.T.G. and S.K. for the PTR-TOF-MS data. L.M.K. and K.G. performed the statistical analyses where K.G. supervised statistical analyses and interpretation. L.M.K. and S.F.M. wrote the manuscript, E.T.G. and K.G. contributed to writing the methods and K.G. contributed to writing results and editing the manuscript.

Competing interests. We declare we have no competing interests.

Funding. This work was supported by the National Science Foundation Doctoral Dissertation Improvement grant (no. NSF DEB 1701915) to L.M.K. and S.F.M., NSF grants to S.F.M. (nos. DEB 1541005 and 1542609); EDEN: Evo-Devo-Eco Network Training Grant to LMK, MicroMorph Cross-Disciplinary Training Grant to L.M.K., the University of Florida's Biology Department grants to L.M.K. and by the Swedish Research Council (2018-06775 to K.G.).

Acknowledgements. We would like to thank Rose McClung and Aurelie Laguerre for technical PTR-TOF-MS support, José-Miguel Ponciano, Javiera Rudolph and Jacqueline L. Sztepanacz for providing advice on statistical analyses, and Sarah B. Carey, Nathan S. Catlin and Charles F. Baer for providing helpful comments on previous drafts of this manuscript. We would also like to thank the anonymous reviewers for their thoughtful and thorough feedback.

References

1. Bateman AJ. 1948 Intra-sexual selection in *Drosophila*. *Heredity* **2**, 349–368. (doi:10.1038/hdy.1948.21)
2. Lessells CM. 2006 The evolutionary outcome of sexual conflict. *Phil. Trans. R. Soc. B* **361**, 301–317. (doi:10.1098/rstb.2005.1795)
3. Chapman T. 2006 Evolutionary conflicts of interest between males and females. *Curr. Biol.* **16**, R744–R754. (doi:10.1016/j.cub.2006.08.020)
4. Bonduriansky R, Chenoweth SF. 2009 Intralocus sexual conflict. *Trends Ecol. Evol.* **24**, 280–288. (doi:10.1016/j.tree.2008.12.005)
5. Parker GA. 1979 Sexual selection and sexual conflict. In *Sexual selection and reproductive competition in insects* (eds MS Blum, NA Blum), pp. 123–166. New York, NY: Academic Press. (doi:10.1016/b978-0-12-108750-0.50010-0)
6. Lande R. 1980 Sexual dimorphism, sexual selection, and adaptation in polygenic characters. *Evolution* **34**, 292. (doi:10.2307/2407393)
7. Kidwell JF, Clegg MT, Stewart FM, Prout T. 1977 Regions of stable equilibria for models of differential selection in the two sexes under random mating. *Genetics* **85**, 171–183.
8. Rice WR. 1992 Sexually antagonistic genes: experimental evidence. *Science* **256**, 1436–1439. (doi:10.1126/science.1604317)
9. Chippindale AK, Gibson JR, Rice WR. 2001 Negative genetic correlation for adult fitness between sexes reveals ontogenetic conflict in *Drosophila*. *Proc. Natl Acad. Sci. USA* **98**, 1671–1675. (doi:10.1073/pnas.98.4.1671)
10. Fry JD. 2010 The genomic location of sexually antagonistic variation: some cautionary comments. *Evolution* **64**, 1510–1516. (doi:10.1111/j.1558-5646.2009.00898.x)
11. Connallon T, Clark AG. 2012 A general population genetic framework for antagonistic selection that accounts for demography and recurrent mutation. *Genetics* **190**, 1477–1489. (doi:10.1534/genetics.111.137117)
12. Connallon T, Clark AG. 2013 Antagonistic versus nonantagonistic models of balancing selection: characterizing the relative timescales and hitchhiking effects of partial selective sweeps. *Evolution* **67**, 908–917. (doi:10.1111/j.1558-5646.2012.01800.x)
13. Barson NJ *et al.* 2015 Sex-dependent dominance at a single locus maintains variation in age at maturity in salmon. *Nature* **528**, 405–408. (doi:10.1038/nature16062)
14. Grieshop K, Arnqvist G. 2018 Sex-specific dominance reversal of genetic variation for fitness. *PLoS Biol.* **16**, e2006810. (doi:10.1371/journal.pbio.2006810)
15. Ruzicka F, Hill MS, Pennell TM, Flis I, Ingleby FC, Mott R, Fowler K, Morrow EH, Reuter M. 2019 Genome-wide sexually antagonistic variants reveal long-standing constraints on sexual dimorphism in fruit flies. *PLoS Biol.* **17**, e3000244. (doi:10.1371/journal.pbio.3000244)
16. Conner J, Via S. 1993 Patterns of phenotypic and genetic correlations among morphological and life-history traits in wild radish, *Raphanus raphanistrum*. *Evolution* **47**, 704–711. (doi:10.1111/j.1558-5646.1993.tb02128.x)
17. Blows MW, Hoffmann AA. 2005 A reassessment of genetic limits to evolutionary change. *Ecology* **86**, 1371–1384. (doi:10.1890/04-1209)
18. Walsh B, Blows MW. 2009 Abundant genetic variation + strong selection = multivariate genetic constraints: a geometric view of adaptation. *Annu. Rev. Ecol. Evol. Syst.* **40**, 41–59. (doi:10.1146/annurev.ecolsys.110308.120232)
19. Hansen TF, Houle D. 2008 Measuring and comparing evolvability and constraint in multivariate characters. *J. Evol. Biol.* **21**, 1201–1219. (doi:10.1111/j.1420-9101.2008.01573.x)
20. Cheng C, Houle D. 2020 Predicting multivariate responses of sexual dimorphism to direct and indirect selection. *Am. Nat.* **196**, 391–405. (doi:10.1086/710353)
21. Wyman MJ, Stinchcombe JR, Rowe L. 2013 A multivariate view of the evolution of sexual dimorphism. *J. Evol. Biol.* **26**, 2070–2080. (doi:10.1111/jeb.12188)
22. Poissant J, Wilson AJ, Coltman DW. 2010 Sex-specific genetic variance and the evolution of sexual dimorphism: a systematic review of cross-sex genetic correlations. *Evolution* **64**, 97–107. (doi:10.1111/j.1558-5646.2009.00793.x)
23. Morrissey MB. 2016 Meta-analysis of magnitudes, differences and variation in evolutionary parameters. *J. Evol. Biol.* **29**, 1882–1904. (doi:10.1111/jeb.12950)

24. Rhen T. 2000 Sex-limited mutations and the evolution of sexual dimorphism. *Evolution* **54**, 37–43. (doi:10.1111/j.0014-3820.2000.tb00005.x)
25. Day T, Bonduriansky R. 2004 Intralocus sexual conflict can drive the evolution of genomic imprinting. *Genetics* **167**, 1537–1546. (doi:10.1534/genetics.103.026211)
26. Fairbairn DJ, Roff DA. 2006 The quantitative genetics of sexual dimorphism: assessing the importance of sex-linkage. *Heredity* **97**, 319–328. (doi:10.1038/sj.hdy.6800895)
27. Lande R, Arnold SJ. 1983 The measurement of selection on correlated characters. *Evolution* **37**, 1210. (doi:10.2307/2408842)
28. Blows MW. 2007 A tale of two matrices: multivariate approaches in evolutionary biology. *J. Evol. Biol.* **20**, 1–8. (doi:10.1111/j.1420-9101.2006.01164.x)
29. Gosden TP, Shastri K-L, Innocenti P, Chenoweth SF. 2012 The b-matrix harbors significant and sex-specific constraints on the evolution of multicharacter sexual dimorphism. *Evolution* **66**, 2106–2116. (doi:10.1111/j.1558-5646.2012.01579.x)
30. Rosenstiel TN, Shortlidge EE, Melnychenko AN, Pankow JF, Eppley SM. 2012 Sex-specific volatile compounds influence microarthropod-mediated fertilization of moss. *Nature* **489**, 431–433. (doi:10.1038/nature11330)
31. Cronberg N, Natcheva R, Hedlund K. 2006 Microarthropods mediate sperm transfer in mosses. *Science* **313**, 1255. (doi:10.1126/science.1128707)
32. Shortlidge EE, Payton AC, Carey SB, McDaniel SF, Rosenstiel TN, Eppley SM. 2020 Microarthropod contributions to fitness variation in the common moss *Ceratodon purpureus*. *bioRxiv*. (doi:10.1101/2020.12.02.408872)
33. Frank SA, Patten MM. 2020 Sexual antagonism leads to a mosaic of X-autosome conflict. *Evolution* **74**, 495–498. (doi:10.1111/evo.13918)
34. McDaniel SF. 2005 Genetic correlations do not constrain the evolution of sexual dimorphism in the moss *Ceratodon purpureus*. *Evolution* **59**, 2353–2361. (doi:10.1111/j.0014-3820.2005.tb00945.x)
35. Vujičić M, Sabovljević A, Sabovljević M. 2011 Axenically culturing the bryophytes: establishment and propagation of the moss *Hypnum cupressiforme* Hedw. (Bryophyta, Hypnaceae) in in vitro conditions. **35**, 71–77.
36. Sabovljević A, Vujičić M, Skorić M, Bajić-Ljubičić J, Sabovljević M. 2012 Axenically culturing the bryophytes: establishment and propagation of the pleurocarpous moss *Thamnobryum alopecurum* Nieuwland ex Gangulee (Bryophyta, Neckeraceae) in in vitro conditions. **44**, 339–344.
37. Cove DJ, Perroud P-F, Charron AJ, McDaniel SF, Khandelwal A, Quatrano RS. 2009 Culturing the moss *Physcomitrella patens*. *Cold Spring Harb. Protoc.* **2009**, db.prot5136. (doi:10.1101/pdb.prot5136)
38. Norrell TE, Jones KS, Payton AC, McDaniel SF. 2014 Meiotic sex ratio variation in natural populations of *Ceratodon purpureus* (Ditrichaceae). *Am. J. Bot.* **101**, 1572–1576. (doi:10.3732/ajb.1400156)
39. Burtscher WP, List MA, Payton AC, McDaniel SF, Carey SB. 2020 Area from image analyses accurately estimates dry-weight biomass of juvenile moss tissue. *bioRxiv* 2020.03.20.000539. (doi:10.1101/2020.03.20.000539)
40. Hadfield JD. 2010 MCMC methods for multi-response generalized linear mixed models: the MCMCglmm R package. *J. Stat. Softw.* **33**, 1210–1226. (doi:10.18637/jss.v033.i02)
41. Grieshop K, Maurizio PL, Arnqvist G, Berger D. 2020 Selection in males purges the standing genetic load on female fitness. *bioRxiv*. 2020.07.20.213132. (doi:10.1101/2020.07.20.213132)
42. Puentes A, Granath G, Ågren J. 2016 Similarity in G matrix structure among natural populations of *Arabidopsis lyrata*. *Evolution* **70**, 2370–2386. (doi:10.1111/evo.13034)
43. Gelman A. 2006 Prior distributions for variance parameters in hierarchical models (comment on article by Browne and Draper). *Bayesian Anal.* **1**, 515–534. (doi:10.1214/06-ba117a)
44. Teplitsky C *et al.* 2014 Assessing multivariate constraints to evolution across ten long-term avian studies. *PLoS ONE* **9**, e90444. (doi:10.1371/journal.pone.0090444)
45. Gelman A, Rubin DB. 1992 Inference from iterative simulation using multiple sequences. *Stat. Sci.* **7**, 457–472. (doi:10.1214/ss/1177011136)
46. Spiegelhalter DJ, Best NG, Carlin BP, van der Linde A. 2002 Bayesian measures of model complexity and fit. *J. R. Stat. Soc. Series B Stat. Methodol.* **64**, 583–639. (doi:10.1111/1467-9868.00353)
47. Aguirre JD, Hine E, McGuigan K, Blows MW. 2014 Comparing G: multivariate analysis of genetic variation in multiple populations. *Heredity* **112**, 21–29. (doi:10.1038/hdy.2013.12)
48. Hine E, Chenoweth SF, Rundle HD, Blows MW. 2009 Characterizing the evolution of genetic variance using genetic covariance tensors. *Phil. Trans. R. Soc. B* **364**, 1567–1578. (doi:10.1098/rstb.2008.0313)
49. Cheverud JM, Marroig G. 2007 Research article comparing covariance matrices: random skewers method compared to the common principal components model. *Genet. Mol. Biol.* **30**, 461–469. (doi:10.1590/S1415-47572007000300027)
50. Steven JC, Delph LF, Brodie ED. 2007 Sexual dimorphism in the quantitative-genetic architecture of floral, leaf, and allocation traits in *Silene latifolia*. *Evolution* **61**, 42–57. (doi:10.1111/j.1558-5646.2007.00004.x)
51. Gosden TP, Chenoweth SF. 2014 The evolutionary stability of cross-sex, cross-trait genetic covariances. *Evolution* **68**, 1687–1697. (doi:10.1111/evo.12398)
52. Sztepanacz JL, Houle D. 2019 Cross-sex genetic covariances limit the evolvability of wing-shape within and among species of *Drosophila*. *Evolution* **73**, 1617–1633. (doi:10.1111/evo.13788)
53. Shaw J, Beer SC. 1999 Life history variation in gametophyte populations of the moss *Ceratodon purpureus* (Ditrichaceae). *Am. J. Bot.* **86**, 512–521. (doi:10.2307/2656812)
54. Barson NJ *et al.* 2015 Sex-dependent dominance at a single locus maintains variation in age at maturity in salmon. *Nature* **528**, 405–408. (doi:10.1038/nature16062)
55. Connallon T, Chenoweth SF. 2019 Dominance reversals and the maintenance of genetic variation for fitness. *PLoS Biol.* **17**, e3000118. (doi:10.1371/journal.pbio.3000118)
56. Carey SB *et al.* 2020 Chromosome fusions shape an ancient UV sex chromosome system. *bioRxiv* 2020.07.03.163634. (doi:10.1101/2020.07.03.163634)
57. Jensen H, Saether BE, Ringsby TH, Tufto J, Griffith SC, Ellegren H. 2003 Sexual variation in heritability and genetic correlations of morphological traits in house sparrow (*Passer domesticus*). *J. Evol. Biol.* **16**, 1296–1307. (doi:10.1046/j.1420-9101.2003.00614.x)
58. Rolff J, Armitage SAO, Coltman DW. 2005 Genetic constraints and sexual dimorphism in immune defense. *Evolution* **59**, 1844. (doi:10.1554/04-747.1)
59. Lewis Z, Wedell N, Hunt J. 2011 Evidence for strong intralocus sexual conflict in the indian meal moth, *Plodia interpunctella*. *Evolution* **65**, 2085–2097. (doi:10.1111/j.1558-5646.2011.01267.x)
60. Berger D, Berg EC, Widegren W, Arnqvist G, Maklakov AA. 2014 Multivariate intralocus sexual conflict in seed beetles. *Evolution* **68**, 3457–3469. (doi:10.1111/evo.12528)
61. Wang X, Werren JH, Clark AG. 2015 Genetic and epigenetic architecture of sex-biased expression in the jewel wasps *Nasonia vitripennis* and *giraulti*. *Proc. Natl Acad. Sci. USA* **112**, E3545–E3554. (doi:10.1073/pnas.1510338112)
62. Ali Balkan M. 2015 Sex-specific fungal communities of the dioicous moss *Ceratodon purpureus*. Thesis, Portland State University, Portland, OR. (doi:10.15760/etd.2654)
63. Holland-Moritz H, Stuart J, Lewis LR, Miller S, Mack MC, McDaniel SF, Fierer N. 2018 Novel bacterial lineages associated with boreal moss species. *Environ. Microbiol.* **20**, 2625–2638. (doi:10.1111/1462-2920.14288)
64. Jean M, Holland-Moritz H, Melvin AM, Johnstone JF, Mack MC. 2020 Experimental assessment of tree canopy and leaf litter controls on the microbiome and nitrogen fixation rates of two boreal mosses. *New Phytol.* **227**, 1335–1349. (doi:10.1111/nph.16611)
65. De Lisle SP, Rowe L. 2017 Disruptive natural selection predicts divergence between the sexes during adaptive radiation. *Ecol. Evol.* **7**, 3590–3601. (doi:10.1002/ece3.2868)
66. De Lisle SP, Goedert D, Reedy AM, Svensson EI. 2018 Climatic factors and species range position predict sexually antagonistic selection across taxa. *Phil. Trans. R. Soc. B* **373**, 20170415. (doi:10.1098/rstb.2017.0415)
67. Kollar L. 2021 Data from: Moss growth, development, morphology, and physiology dataset and code. Dryad Digital Repository. (https://doi.org/10.5061/dryad.59zw3r266)